Eidgenössische Technische Hochschule Zürich
Swiss Federal Institute of Technology Zurich

Seminar for Applied Mathematics

Reconstructing fine details of small objects by using plasmonic spectroscopic data. Part II: The strong interaction regime

H. Ammari and M. Ruiz and S. Yu and H. Zhang

Research Report No. 2017-55
December 2017

Seminar für Angewandte Mathematik
Eidgenössische Technische Hochschule
CH-8092 Zürich
Switzerland

Funding: The work of Hai Zhang was supported by HK RGC grant ECS 26301016 and startup fund R9355 from HKUST.

Reconstructing fine details of small objects by using plasmonic spectroscopic data. Part II: The strong interaction regime

Habib Ammari* Matias Ruiz† Sanghyeon Yu † Hai Zhang‡

Abstract

This paper is concerned with the inverse problem of reconstructing a small object from far field measurements by using the field interaction with a plasmonic particle which can be viewed as a passive sensor. It is a follow-up of the work [H. Ammari et al., Reconstructing fine details of small objects by using plasmonic spectroscopic data, SIAM J. Imag. Sci., to appear], where the intermediate interaction regime was considered. In that regime, it was shown that the presence of the target object induces small shifts to the resonant frequencies of the plasmonic particle. These shifts, which can be determined from the far field data, encodes the contracted generalized polarization tensors of the target object, from which one can perform reconstruction beyond the usual resolution limit. The main argument is based on perturbation theory. However, the same argument is no longer applicable in the strong interaction regime as considered in this paper due to the large shift induced by strong field interaction between the particles. We develop a novel technique based on conformal mapping theory to overcome this difficulty. The key is to design a conformal mapping which transforms the two particle system into a shell-core structure, in which the inner dielectric core corresponds to the target object. We show that a perturbation argument can be used to analyze the shift in the resonant frequencies due to the presence of the inner dielectric core. This shift also encodes information of the contracted polarization tensors of the core, from which one can reconstruct its shape, and hence the target object. Our theoretical findings are supplemented by a variety of numerical results based on an efficient optimal control algorithm. The results of this paper make the mathematical foundation for plasmonic sensing complete.

Mathematics Subject Classification (MSC2000): 35R30, 35C20.

Keywords: plasmonic sensing, superresolutoion, far-field measurement, generalized polarization tensors.

1 Introduction

The inverse problem of reconstructing fine details of small objects by using far-field measurements is severally ill-posed. There are two fundamental reasons for this: the diffraction limit and the low signal to noise ratio in the measurements.

*Department of Mathematics, ETH Zürich, Rämistrasse 101, CH-8092 Zürich, Switzerland (habib.ammari@math.ethz.ch, sanghyeon.yu@sam.math.ethz.ch).

†Department of Mathematics and Applications, Ecole Normale Supérieure, 45 Rue d'Ulm, 75005 Paris, France (matias.ruiz@ens.fr).

‡Department of Mathematics, HKUST, Clear Water Bay, Kowloon, Hong Kong (haizhang@ust.hk). The work of Hai Zhang was supported by HK RGC grant ECS 26301016 and startup fund R9355 from HKUST.

Motivated by plasmonic sensing in molecular biology (see [30] and the references therein), we developed a new methodology to overcome the ill-posedness of this inverse problem in [10]. The key idea is to use a plasmonic particle to interact with the target object and to propagate its near field information into far-field in terms of the shifts in the plasmonic resonant frequencies. This plasmonic particle can be viewed as a passive sensor in the simplest form. For such a plasmonic-particle sensor, one of the most important characterization is the plasmon resonant frequencies associated with it. These resonant frequencies depend not only on the electromagnetic properties of the particle and its size and shape [7, 9, 22, 28], but also on the electromagnetic properties of the environment [7, 22, 23]. It is the last property which enables the sensing application of plasmonic particles.

In [10], the target object is modeled by a dielectric particle whose size is much smaller than that of the sensing plamsonic particle. The intermediate regime where the distance of the two particles is comparable to the size of the plasmonic particle was investigated. it was shown the shifts of the plasmonic resonant frequencies of the plasmonic particle is small and a perturbation argument can be used to derive their asymptotic. Based on these asymptotic formulas, one can obtain their explicit dependence on the generalized polarization tensors of the target particle from which one can perform its reconstruction. However, when the distance between the particles decreases, their interactions increases and the induced shifts increase in magnitude as well. The perturbation argument will cease to work at certain threshold distance, and the characterization for the shifts of resonant frequencies in terms of information of the target particle becomes more complicated.

In this paper, we aim to extend the above investigation to the strong interaction regime where the distance of between the two particles is comparable to the size of the small particle. In this regime, the near field interactions are strong and the induced large shifts in plasmonic resonant frequencies cannot be analyzed by a perturbation argument. In order to overcome this difficulty, we develop a novel technique based on conforming mapping theory. The key is to design a conformal mapping which transforms the two-particle system into a shell-core structure, in which the inner dielectric core corresponds to the target object. We showed that a perturbation argument can be used to analyze the shift in the resonance frequencies due to the presence of the inner dielectric core. This shift also encodes information on the contracted polarization tensors of the core, from which one can reconstruct its shape, and hence the target object. The results of this paper make the mathematical foundation for plasmonic sensing complete.

We remark that the above idea of plasmonic sensing is closely related to that of super-resolution in resonant media, where the basic idea is to propagate the near field information into the far field through certain near field coupling with subwavelength resonators. In a recent series of papers [11, 12, 13], we have shown mathematically how to realize this idea by using weakly coupled subwavelength resonators and achieve super-resolution and super-focusing. The key is that the near field information of sources can be encoded in the subwavelength resonant modes of the system of resonators through the near field coupling. These excited resonant modes can propagate into the far-field and thus makes the super-resolution from far field measurements possible.

This paper is organized as follows. In Section 2, we provide basic results on layer potentials and then explain the concept of plasmonic resonances and the (contracted) generalized polarization tensors. In Section 3, we consider the forward scattering problem of the incident field interaction with a system composed of an dielectric particle and a plasmonic particle. We derive the asymptotic of the scattered field in the case of strong regime. In Section 4, we consider the inverse problem of reconstructing the geometry of the dielectric particle. This is done by constructing the contracted generalized polarization tensors of the target particle through the resonance shifts induced to the plasmonic particle. We provide numerical examples to justify our theoretical results and to illustrate the performances of the proposed optimal control reconstruction scheme.

2 Preliminaries

2.1 Layer potentials

We recall some basic of layer potential theory that are needed for subsequent analysis. We refer to [4] for more details. We denote by $G(x,y)$ the Green function for the Laplacian in the free space $\mathbb{R}^2$, i.e.

$$G(x,y) = \frac{1}{2\pi}\log|x-y|.$$

Let D be a domain $\mathbb{R}^2$ with $\mathcal{C}^{1,\eta}$ boundary for some $\eta > 0$, and let $\nu(x)$ be the outward normal for $x \in \partial D$.

The single layer potential $\mathcal{S}_D$ associated with D is defined by

$$\mathcal{S}_D[\varphi](x) = \int_{\partial D} G(x,y)\varphi(y)d\sigma(y), \quad x \in \mathbb{R}^2,$$

and the Neumann-Poincaré (NP) operator $\mathcal{K}_D^*$ by:

$$\mathcal{K}_D^*[\varphi](x) = \int_{\partial D} \frac{\partial G}{\partial \nu(x)}(x,y)\varphi(y)d\sigma(y), \quad x \in \partial D.$$

The following jump relations hold:

$$\mathcal{S}_D[\varphi]\big|_+ = \mathcal{S}_D[\varphi]\big|_-, \tag{2.1}$$

$$\frac{\partial \mathcal{S}_D[\varphi]}{\partial \nu}\Big|_\pm = (\pm\frac{1}{2}I + \mathcal{K}_D^*)[\varphi]. \tag{2.2}$$

Here, the subscripts + and − indiciate the limits from ouside and inside D, respectively.

Let $H^{1/2}(\partial D)$ be the usual Sobolev space and let $H^{-1/2}(\partial D)$ be its dual space with respect to the duality pairing $(\cdot,\cdot)_{-\frac{1}{2},\frac{1}{2}}$. We denote by $H_0^{-1/2}(\partial D)$ the collection of all $\varphi \in H^{-1/2}(\partial D)$ such that $(\varphi, 1)_{-\frac{1}{2},\frac{1}{2}} = 0$.

The NP operator is bounded from $H^{-1/2}(\partial D)$ to $H^{-1/2}(\partial D)$. Moreover, the operator $\lambda I - \mathcal{K}_D^* : L^2(\partial D) \to L^2(\partial D)$ is invertible for any $|\lambda| > 1/2$. Although the NP operator is not self-adjoint on $L^2(\partial D)$, it can be symmetrized on $H_0^{-1/2}(\partial D)$ with a proper inner product [14, 7]. In fact, let $\mathcal{H}^*(\partial D)$ be the space $H_0^{-1/2}(\partial D)$ equipped with the inner product $(\cdot,\cdot)_{\mathcal{H}^*(\partial D)}$ defined by

$$(\varphi,\psi)_{\mathcal{H}^*(\partial D)} = -(\varphi, \mathcal{S}_D[\psi])_{-\frac{1}{2},\frac{1}{2}},$$

for $\varphi, \psi \in H^{-1/2}(\partial D)$. Then using the Plemelj's symmetrization principle,

$$\mathcal{S}_D \mathcal{K}_D^* = \mathcal{K}_D \mathcal{S}_D,$$

it can be shown that the NP operator $\mathcal{K}_D^*$ is self-adjoint in $\mathcal{H}^*$ with the inner product $(\cdot, \cdot)_{\mathcal{H}^*(\partial D)}$. Since $\mathcal{K}_D^*$ is also compact, it admits the following spectral decomposition in $\mathcal{H}^*$,

$$\mathcal{K}_D^* = \sum_{j=1}^{\infty} \lambda_j (\cdot, \varphi_j)_{\mathcal{H}^*} \varphi_j, \tag{2.3}$$

where λ_j are the eigenvalues of $\mathcal{K}_D^*$ and φ_j are their associated eigenfunctions. Note that $|\lambda_j| < 1/2$ for all $j \geq 1$.

2.2 Plasmonic resonance

We are interested in the frequency regime where plasmonic resonances occur. In such a regime, the wavelength of the incident field is much greater than the size of the plasmonic particle. To further simplify the analysis and better illustrate the main idea, we use the quasi-static approximation (by assuming the incident wavelength to be infinite) to model the interaction. More precisely, let D represent a plasmonic particle with permittivity ε_D embedded in the homogenous space $\mathbb{R}^2$ with permittivity ε_m. We consider the following transmission problem with given incident field H which is harmonic:

$$\begin{cases} \nabla \cdot (\varepsilon \nabla u) = 0 & \text{in } \mathbb{R}^2, \\ u - u^i = O(|x|^{-1}) & \text{as } |x| \to \infty, \end{cases} \tag{2.4}$$

where $\varepsilon = \varepsilon_D \chi(D) + \varepsilon_m \chi(\mathbb{R}^2 \backslash \overline{D})$, and $\chi(D)$ and $\chi(\mathbb{R}^2 \backslash \overline{D})$ are the characteristic functions of D and $\mathbb{R}^2 \backslash \overline{D}$, respectively. The total field u outside of D can be represented by

$$u = u^i + \mathcal{S}_D[\varphi]\,, \tag{2.5}$$

where the density φ satisfies the boundary integral equation

$$(\lambda I - \mathcal{K}_D^*)[\varphi] = \frac{\partial u^i}{\partial \nu}\Big|_{\partial D}. \tag{2.6}$$

Here, λ is given by

$$\lambda = \frac{\varepsilon_D + \varepsilon_m}{2(\varepsilon_D - \varepsilon_m)}. \tag{2.7}$$

Contrary to ordinary dielectric particles, the permittivity ε_D of the plasmonic particle has negative real parts. In fact, ε_D depends on the operating frequency ω and can be modeled by the following Drude's model

$$\varepsilon_D = \varepsilon_D(\omega) = 1 - \frac{\omega_p^2}{\omega(\omega + i\gamma)}, \tag{2.8}$$

where $\omega_p > 0$ is called the plasma frequency and $\gamma > 0$ is the damping parameter. Since the parameter γ is typically very small, $\varepsilon_D(\omega)$ has a small imaginary part.

Now we discuss the plasmonic resonances. By applying the spectral decomposition (2.3) of

$\mathcal{K}_D^*$ to the integral equation (2.6), we obtain

$$\varphi = \sum_{j=1}^{\infty} \frac{(\frac{\partial u^i}{\partial \nu}, \varphi_j)_{\mathcal{H}^*(\partial D)}}{\lambda_D - \lambda_j} \varphi_j. \tag{2.9}$$

Recall that λ_j are eigenvalues $\mathcal{K}_D^*$ and they satisfy the condition that $|\lambda_j| < 1/2$. For $\omega < \omega_p$, $\mathrm{Re}\{\varepsilon_D(\omega)\}$ can take negative values. Then it holds that $|\mathrm{Re}\{\lambda(\omega)\}| < 1/2$. If there exists a frequency, say ω_j, such that $\lambda(\omega_j)$ is close to an eigenvalue λ_j of the NP operator and their difference is locally minimized. Provided that $(\frac{\partial u^i}{\partial \nu}, \varphi_j)_{\mathcal{H}^*(\partial D)} \neq 0$, the eigenmode φ_j in (2.9) will be fully excited and it dominates over other modes. As a result, the scattered field $u - u^i$ will show a pronounced peak at the frequency ω_j. This phenomenon is called the plasmonic resonance and ω_j is called the plasmonic resonant frequency.

When D is an ellipse of the form

$$D = \Big\{(x, y) \in \mathbb{R}^2 : \frac{x^2}{a^2} + \frac{y^2}{b^2} \leq 1\Big\}, \tag{2.10}$$

for some constants a, b with $a < b$, we can compute the eigenvalues of the NP operator $\mathcal{K}_D^*$ explicitly. In fact, they are given by

$$\pm\frac{1}{2}\Big(\frac{b-a}{b+a}\Big)^j, \quad j = 1, 2, 3, \cdots .$$

If $a = b$, then D is a circular disk of radius a. In this case, zero is the only eigenvalue.

2.3 Contracted generalized polarization tensors

In this subsection, we explain the concept of the generalized polarization tensors (GPTs). The scattered field $u - u^i$ has the following far-field behavior [4, p. 77]

$$(u - u^i)(x) = \sum_{|\alpha|, |\beta| \leq 1} \frac{1}{\alpha!\beta!} \partial^\alpha u^i(0) M_{\alpha\beta}(\lambda, D) \partial^\beta G(x), \quad |x| \to +\infty, \tag{2.11}$$

where $M_{\alpha\beta}(\lambda, D)$ is given by

$$M_{\alpha\beta}(\lambda, D) := \int_{\partial D} y^\beta (\lambda I - \mathcal{K}_D^*)^{-1}[\frac{\partial x^\alpha}{\partial \nu}](y)\, d\sigma(y), \qquad \alpha, \beta \in \mathbb{N}^2.$$

Here, the coefficient $M_{\alpha\beta}(\lambda, D)$ is called the *generalized polarization tensor* [4].

For a positive integer m, let $P_m(x)$ be the complex-valued polynomial

$$P_m(x) = (x_1 + ix_2)^m = r^m \cos m\theta + ir^m \sin m\theta, \tag{2.12}$$

where we have used the polar coordinates $x = re^{i\theta}$.

We define the *contracted generalized polarization tensors* (CGPTs) to be the following linear combinations of generalized polarization tensors using the polynomials in (2.12):

$$\begin{aligned} M^{cc}_{m,n}(\lambda,D) &= \int_{\partial D} \mathrm{Re}\{P_n\}(\lambda I-\mathcal{K}^*_D)^{-1}[\tfrac{\partial \mathrm{Re}\{P_m\}}{\partial\nu}]\, d\sigma, \\ M^{cs}_{m,n}(\lambda,D) &= \int_{\partial D} \mathrm{Im}\{P_n\}(\lambda I-\mathcal{K}^*_D)^{-1}[\tfrac{\partial \mathrm{Re}\{P_m\}}{\partial\nu}]\, d\sigma, \\ M^{sc}_{m,n}(\lambda,D) &= \int_{\partial D} \mathrm{Re}\{P_n\}(\lambda I-\mathcal{K}^*_D)^{-1}[\tfrac{\partial \mathrm{Im}\{P_m\}}{\partial\nu}]\, d\sigma, \\ M^{ss}_{m,n}(\lambda,D) &= \int_{\partial D} \mathrm{Im}\{P_n\}(\lambda I-\mathcal{K}^*_D)^{-1}[\tfrac{\partial \mathrm{Im}\{P_m\}}{\partial\nu}]\, d\sigma. \end{aligned} \tag{2.13}$$

We remark that CGPTs defined above encodes useful information about the shape of the particle D and can be used for its reconstruction. See [4, 3, 5, 6] for more details.

For convenience, we introduce the following notation. We denote

$$M_{m,n}(\lambda,D) \quad = \quad \begin{pmatrix} M^{cc}_{m,n}(\lambda,D) & M^{cs}_{m,n}(\lambda,D) \\ M^{sc}_{m,n}(\lambda,D) & M^{ss}_{m,n}(\lambda,D) \end{pmatrix}.$$

When $m=n=1$, the matrix $M(\lambda,D) := M_{1,1}(\lambda,D)$ is called the *first order polarization tensor*. Specifically, we have

$$M(\lambda,D)_{lm} = \int_{\partial D} y_j(\lambda I-\mathcal{K}^*_D)^{-1}[\nu_i](y)\, d\sigma(y), \quad l,m=1,2.$$

It is worth mentioning that the following symmetry holds (see [4]):

$$M_{mn} = M^T_{nm}.$$

Since, from (2.11), we have

$$(u-u^i)(x) = \frac{\nabla u^i\cdot M(\lambda,D)x}{|x|^2} + O(|x|^{-2}), \quad \text{as } |x|\to\infty,$$

the first order polarization tensor $M(\lambda,D)$ determines the dominant term in the far-field expansion of the scattered field $u-u^i$.

To see the plasmonic resonance in the far field, we represent $M(\lambda,D)$ in a spectral form. By (2.3), we have

$$M(\lambda,D)_{lm} = \sum_{j=1}^{\infty} \frac{(y_m,\varphi_j)_{-\frac{1}{2},\frac{1}{2}}(\varphi_j,\nu_l)_{\mathcal{H}^*(\partial D)}}{\lambda-\lambda_j}.$$

If D is the ellipse given by (2.10), then we have the explicit formula

$$M(\lambda,D) = \begin{pmatrix} \frac{\pi ab}{\lambda-\frac{1}{2}\frac{a-b}{a+b}} & 0 \\ 0 & \frac{\pi ab}{\lambda+\frac{1}{2}\frac{a-b}{a+b}} \end{pmatrix}. \tag{2.14}$$

Formula (2.14) indicates that the plasmonic resonance occurs only if λ is close to $\frac{1}{2}\frac{a-b}{a+b}$ or $-\frac{1}{2}\frac{a-b}{a+b}$.

3 The forward problem

We consider a system composed of a dielectric particle and a plasmonic particle embedded in a homogeneous medium. The target dielectric particle and the plasmonic particle occupy a bounded and simply connected domain $D_1 \subset \mathbb{R}^2$ and $D_2 \subset \mathbb{R}^2$ of class $\mathcal{C}^{1,\alpha}$ for some $0 < \alpha < 1$, respectively. We further assume that D_1 contains the origin. We denote the permittivity of the dielectric particle D_1 and the plasmonic particle D_2 by ε_1 and ε_2, respectively. The permittivity of the background medium is denoted by ε_m. In other words, the permittivity distribution ε is given by

$$\varepsilon := \varepsilon_1 \chi(D_1) + \varepsilon_2 \chi(D_2) + \varepsilon_m \chi(\mathbb{R}^2 \backslash (\overline{D_1 \cup D_2})).$$

As in Subsection 2.2, the permittivity ε_2 of the plasmonic particle depends on the operating frequency and is modeled as

$$\varepsilon_2 = \varepsilon_2(\omega) = 1 - \frac{\omega_p^2}{\omega(\omega + i\gamma)}.$$

For ease of notation, we denote

$$\lambda_{D_j} = \frac{\varepsilon_j + \varepsilon_m}{2(\varepsilon_j - \varepsilon_m)}, \quad j = 1, 2.$$

The total electric potential u satisfies the following equation:

$$\begin{cases} \nabla \cdot (\varepsilon \nabla u) = 0 & \text{in } \mathbb{R}^2 \backslash (\partial D_1 \cup \partial D_2), \\ u|_+ = u|_- & \text{on } \partial D_1 \cup \partial D_2, \\ \varepsilon_m \dfrac{\partial u}{\partial \nu}\Big|_+ = \varepsilon_1 \dfrac{\partial u}{\partial \nu}\Big|_- & \text{on } \partial D_1, \\ \varepsilon_m \dfrac{\partial u}{\partial \nu}\Big|_+ = \varepsilon_2 \dfrac{\partial u}{\partial \nu}\Big|_- & \text{on } \partial D_2, \\ (u - u^i)(x) = O(|x|^{-1}), & \text{as } |x| \to \infty, \end{cases} \tag{3.1}$$

where $u^i(x) = d \cdot x$ is the incident potential with a constant vector $d \in \mathbb{R}^2$.

3.1 Boundary integral formulation

We derive a layer potential representation of the total field u to (3.1) in this section. We first denote by u_{D_1} the total field resulting from the incident field u^i and the ordinary particle D_1 (without the plasmonic particle D_2). Then u_{D_1} has the following representation:

$$u_{D_1}(x) = u^i(x) + \mathcal{S}_{D_1} \left(\lambda_{D_1} Id - \mathcal{K}^*_{D_1} \right)^{-1} [\frac{\partial u^i}{\partial \nu_1}](x), \quad \text{for } x \in \mathbb{R}^2 \backslash \overline{D_1}.$$

We next introduce the Green function $G_{D_1}(\cdot, y)$ for the medium with permittivity distribution $\varepsilon_{D_1} \chi(D_1) + \varepsilon_m \chi(\mathbb{R}^2 \backslash \overline{D_1})$. More precisely, $G_{D_1}(\cdot, y)$ satisfies the following equation

$$\nabla_x \cdot \big((\varepsilon_{D_1} \chi(D_1) + \varepsilon_m \chi(\mathbb{R}^2 \backslash \overline{D_1})) \nabla_x G_{D_1}(x, y) \big) = \delta(x - y).$$

One can show that

$$G_{D_1}(x,y) = G(x,y) + \mathcal{S}_{D_1}\left(\lambda_{D_1} Id - \mathcal{K}^*_{D_1}\right)^{-1}\left[\frac{\partial}{\partial \nu} G(\cdot, y)\right](x) \quad \text{for } x, y \in \mathbb{R}^2 \backslash \overline{D_1}. \tag{3.2}$$

Using G_{D_1}, we define layer potential $\mathcal{S}_{D_2,D_1}$ by

$$\mathcal{S}_{D_2,D_1}[\varphi](x) = \int_{\partial D_2} G_{D_1}(x,y)\varphi(y) d\sigma(y).$$

The total potential u can then be represented in the following form:

$$u = u_{D_1} + \mathcal{S}_{D_2,D_1}[\psi], \quad x \in \mathbb{R}^2 \backslash \overline{D_2}, \tag{3.3}$$

where density ψ satisfies the following boundary integral equation

$$\left(\lambda_{D_2} Id - \mathcal{A}\right)[\psi] = \frac{\partial u_{D_1}}{\partial \nu_2} \tag{3.4}$$

with

$$\mathcal{A} = \mathcal{K}^*_{D_2} - \frac{\partial}{\partial \nu_2} \mathcal{S}_{D_1}\left(\lambda_{D_1} Id - \mathcal{K}^*_{D_1}\right)^{-1} \frac{\partial \mathcal{S}_{D_2}[\cdot]}{\partial \nu_1}.$$

We note that the equation (3.4) is written in the form

$$\left(\mathcal{A}_{D_2,0} + \mathcal{A}_{D_2,1}\right)[\psi] = \frac{\partial u_{D_1}}{\partial \nu_2}, \tag{3.5}$$

where

$$\begin{aligned} \mathcal{A}_{D_2,0} &= \lambda_{D_2} Id - \mathcal{K}^*_{D_2}, \\ \mathcal{A}_{D_2,1} &= \frac{\partial}{\partial \nu_2} \mathcal{S}_{D_1}\left(\lambda_{D_1} Id - \mathcal{K}^*_{D_1}\right)^{-1} \frac{\partial \mathcal{S}_{D_2}[\cdot]}{\partial \nu_1}. \end{aligned} \tag{3.6}$$

3.2 Strong interaction regime and conformal transformation

We assume the following condition on the sizes of the particles D_1 and D_2.

Condition 1. *The plasmonic particle D_2 has size of order one; the dielectric particle D_1 has size of order $\delta \ll 1$.*

Definition 3.1 (**Strong interaction regime**). *We say that the small dielectric particle D_1 is in the strong regime with respect to the plasmonic particle D_2 if there exist positive constants C_1 and C_2 such that $C_1 < C_2$ and*

$$C_1 \delta \leq \operatorname{dist}(D_1, D_2) \leq C_2 \delta.$$

Definition 3.1 says that the dielectric particle D_1 is closely located to the plasmonic particle D_2 with a separation distance of order δ.

In our recent paper [10], the intermediate interaction regime is considered. The key observation is that the distance between D_1 and D_2 is assumed to be of order one. The operator $\mathcal{A}_{D_2,1}$ in the integral equation (3.5) can be considered as a small perturbation to the operator $\mathcal{A}_{D_2,0}$.

However, in the strong interaction regime, the operator $\mathcal{A}_{D_2,1}$ is no longer small compared to the latter. As a consequence, the perturbation theory is not applicable and it becomes challenging to analyze the interaction between the particles .

We now introduce a method to tackle this issue by using conformal mapping technique. Let B_1 be a circular disks containing the dielectric particle D_1 with radius r_1 of order δ. We assume the plasmonic particle D_2 is a circular disk with radius r_2. For convenience, we denote D_2 by B_2. We emphasize that the shape of D_1 is unknown. We let d to be the distance between the two disks B_1 and B_2, *i.e.*,

$$d = \operatorname{dist}(B_1, B_2).$$

By the assumption, d is of order δ.

Let R_j be the reflection with respect to ∂B_j and let $\mathbf{p}_1$ and $\mathbf{p}_2$ be the unique fixed points of the combined reflections $R_1 \circ R_2$ and $R_2 \circ R_1$, respectively. Let $\mathbf{n}$ be the unit vector in the direction of $\mathbf{p}_2 - \mathbf{p}_1$. We set $(x, y) \in \mathbb{R}^2$ to be the Cartesian coordinates such that $\mathbf{p} = (\mathbf{p}_1 + \mathbf{p}_2)/2$ is the origin and the x-axis is parallel to $\mathbf{n}$. Then one can see that $\mathbf{p}_1$ and $\mathbf{p}_2$ can be written as

$$\mathbf{p}_1 = (-a, 0) \quad \text{and} \quad \mathbf{p}_2 = (a, 0), \tag{3.7}$$

where the constant a is given by

$$a = \frac{\sqrt{d}\sqrt{(2r_1 + d)(2r_2 + d)(2r_1 + 2r_2 + d)}}{2(r_1 + r_2 + d)}. \tag{3.8}$$

Then the center $\mathbf{c}_i$ of B_i $(i = 1, 2)$ is given by

$$\mathbf{c}_i = \Big((-1)^i \sqrt{r_i^2 + a^2}, 0\Big). \tag{3.9}$$

Define the conformal transformation Φ by

$$\zeta = \Phi(z) = \frac{z + a}{z - a}, \quad z = x + iy.$$

In other words,

$$z = \Phi^{-1}(\zeta) = a\frac{\zeta + 1}{\zeta - 1}.$$

We also define

$$s_j = (-1)^j \sinh^{-1}(a/r_j), \quad j = 1, 2,$$

and the two disks $\widetilde{B}_1$ and $\widetilde{B}_2$ by

$$\widetilde{B}_1 = \{|\zeta| < \tilde{r}_j\}, \quad \tilde{r}_j = \exp(s_j),\ j = 1, 2.$$

It can be shown that, in the ζ-plane, the disks B_1 and B_2 are transformed to

$$\Phi(B_1) = \widetilde{B}_1 = \{|\zeta| < \tilde{r}_1\},$$

and

$$\Phi(B_2) = \mathbb{R}^2 \setminus \overline{\widetilde{B}_2} = \{|\zeta| > \tilde{r}_2\}.$$

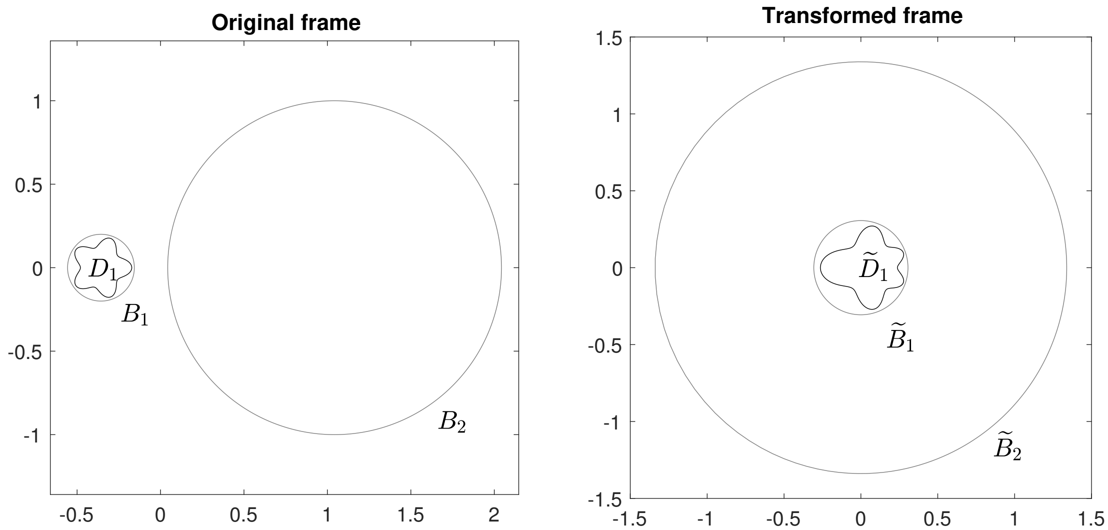

Figure 1: (left) original configuration and (right) transformed one by the conformal map Φ

One can check that $\tilde{r}_1 < 1$ and $\tilde{r}_2 > 1$. The exterior region $\mathbb{R}^2 \setminus \overline{B_1 \cup B_2}$ becomes a shell region between $\partial\widetilde{B}_1$ and $\partial\widetilde{B}_2$ in the ζ-plane:

$$\Phi(\mathbb{R}^2 \setminus \overline{B_1 \cup B_2}) = \widetilde{B}_2 \setminus \overline{\widetilde{B}_1} = \{\tilde{r}_1 < |\zeta| < \tilde{r}_2\}.$$

To illustrate the geomtery, in Figure 1,we show an example for the configuration of a system of a small dielectric particle D_1 and a plasmonic particle B_2. We also show its transformed geometry by the conformal map Φ. We set $\delta = 0.2$, $r_1 = \delta$, $r_2 = 1$ and $d = \delta$.

It is worth mentioning that the shape of the transformed domain $\widetilde{D}_1$ strongly depends on the ratio between d and δ but is independent of δ itself. Suppose that $d = c\delta$ for some $c > 0$. If c is of order one, then the shape of $\widetilde{D}_1$ is almost the same as that of D_1. On the contrary, if c is too small, then the shape of $\widetilde{D}_1$ is highly distorted. See Figure 2.

3.3 Boundary integral formualtion in the transformed domain

Let us define $\tilde{u}(\zeta) = u(\Phi^{-1}(\zeta))$ and $\tilde{u}^i(\zeta) = u^i(\Phi^{-1}(\zeta))$. Then, since the mapping Φ is conformal, $\tilde{u}$ and $\tilde{u}^i$ are harmonic in the ζ-plane. Moreover, the transmission conditions for $\tilde{u}$ are preserved.

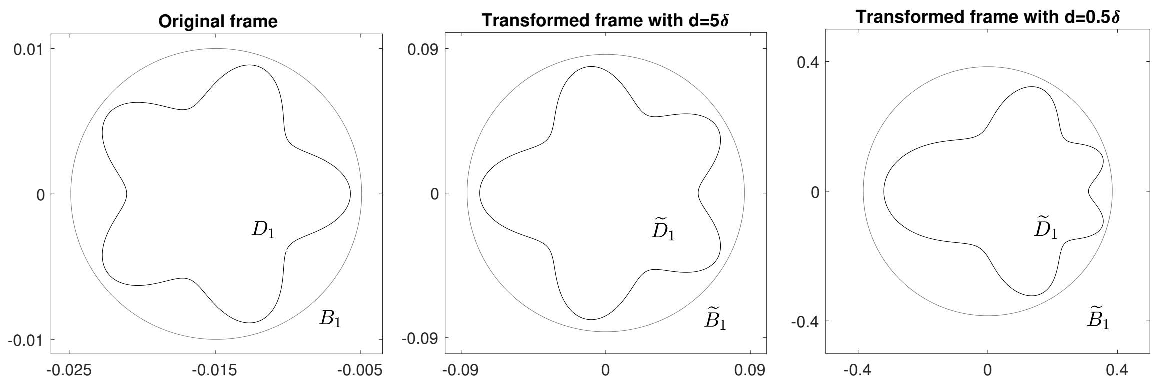

Figure 2: (left) original configuration (center) the transformed one with $d = 5\delta$ (right) the same but with $d = 0.5\delta$. We set $r_1 = \delta$, $r_2 = 1$ and $\delta = 0.01$.

In fact, the transformed potential $\tilde{u}$ satisfies the following equations:

$$\begin{cases} \nabla\cdot(\tilde{\varepsilon}\nabla\tilde{u}) = 0 & \text{in } \mathbb{R}^2\backslash(\partial\widetilde{D}_1\cup\partial\widetilde{D}_2), \\ \tilde{u}|_+ = \tilde{u}|_- & \text{on } \partial\widetilde{D}_1\cup\partial\widetilde{D}_2, \\ \varepsilon_m\dfrac{\partial\tilde{u}}{\partial\nu}\Big|_+ = \varepsilon_1\dfrac{\partial\tilde{u}}{\partial\nu}\Big|_- & \text{on } \partial\widetilde{D}_1, \\ \varepsilon_2\dfrac{\partial\tilde{u}}{\partial\nu}\Big|_+ = \varepsilon_m\dfrac{\partial\tilde{u}}{\partial\nu}\Big|_- & \text{on } \partial\widetilde{D}_2, \\ (\tilde{u}-\tilde{u}^i)(\zeta) = O(|\zeta-(1,0)|) & \text{as } \zeta\to(1,0), \end{cases} \tag{3.10}$$

where the transformed permittivity distribution $\tilde{\varepsilon}$ is given by

$$\tilde{\varepsilon} = \varepsilon_1\chi(\widetilde{D}_1) + \varepsilon_2\chi(\mathbb{R}^2\setminus\widetilde{D}_2) + \varepsilon_m\chi(\widetilde{D}_2\setminus\overline{\widetilde{D}_1}).$$

Note that the transformed problem looks similar to the original one, even though the geometry of the particles is of a completely different nature. As δ goes to zero, the radii $\tilde{r}_1$ and $\tilde{r}_2$ have the following asymptotic properties:

$$\tilde{r}_1 = \tilde{r}_1^0 + O(\delta), \quad \tilde{r}_2 = 1 + O(\delta)$$

for some $0 < r_1^0 < 1$ independent of δ. Hence, in contrast to the original problem, the transformed boundaries $\partial\widetilde{B}_1$ and $\partial\widetilde{B}_2$ $(= \partial\widetilde{D}_2)$ are not close to touching. Moreover, they share the same center (see Figure 1). This will enable us to analyze more deeply the spectral nature of the problem.

Now we represent the solution to the transformed problem using the layer potentials. By applying a similar procedure as the one used for (3.6), we can obtain the following representation:

$$\tilde{u} = (\text{const.}) + u_{\widetilde{D}_1} + \mathcal{S}_{\widetilde{D}_2,\widetilde{D}_1}[\widetilde{\psi}], \quad x\in\mathbb{R}^2. \tag{3.11}$$

Here, the constant term is needed to satisfy the boundary condition at infinity in (3.10). The density function $\widetilde{\psi}$ satisfies the following boundary integral equation:

$$\left(\lambda_{D_2} I - \widetilde{\mathcal{A}}\right)[\widetilde{\psi}] = \frac{\partial \tilde{u}_{\widetilde{D}_1}}{\partial \nu_2}, \tag{3.12}$$

where

$$\begin{aligned} \widetilde{\mathcal{A}} &= \mathcal{K}^*_{\widetilde{D}_2} - \frac{\partial}{\partial \nu_2} \mathcal{S}_{\widetilde{D}_1} \left(\lambda_{D_1} I - \mathcal{K}^*_{\widetilde{D}_1}\right)^{-1} \frac{\partial \mathcal{S}_{\widetilde{D}_2}[\cdot]}{\partial \nu_1}, & (3.13) \\ \tilde{u}_{\widetilde{D}_1} &= \tilde{u}^i + \mathcal{S}_{\widetilde{D}_1} \left(\lambda_{D_1} I - \mathcal{K}^*_{\widetilde{D}_1}\right)^{-1} \left[\frac{\partial \tilde{u}^i}{\partial \nu_1}\right]. & (3.14) \end{aligned}$$

Lemma 3.1. *The following relation between $\mathcal{A}$ and $\widetilde{\mathcal{A}}$ holds*

$$\langle \phi, \mathcal{A}[\psi] \rangle_{\mathcal{H}^*(\partial D_2)} = \langle \widetilde{\phi}, \widetilde{\mathcal{A}}[\widetilde{\psi}] \rangle_{\mathcal{H}^*(\partial \widetilde{D}_2)}, \tag{3.15}$$

where $\phi, \psi \in \mathcal{H}^*(\partial D_2)$ and $\widetilde{\phi} = \phi \circ \Phi^{-1}, \widetilde{\psi} = \psi \circ \Phi^{-1}$.

Proof. By the conformality of the map Φ, the single layer potentials $\mathcal{S}_{D_2}[\phi]$ and $\mathcal{S}_{\widetilde{D}_2}[\widetilde{\phi}] \circ \Phi$ are identical up to an additive constant, whence (3.15) follows.

3.4 Computation of the operator $\widetilde{\mathcal{A}}$ and its spectral properties

Here we compute the operator $\widetilde{\mathcal{A}}$. Note that $\widetilde{\mathcal{A}}$ is an operator which maps $\mathcal{H}^*(\partial \widetilde{D}_2)$ onto $\mathcal{H}^*(\partial \widetilde{D}_2)$. Since $\partial \widetilde{D}_2$ is a circle, we use the Fourier basis for $\mathcal{H}^*(\partial \widetilde{D}_2)$. Let (r, θ) be the polar coordinates in the ζ-plane, *i.e.*, $\zeta = re^{i\theta}$. We define

$$\varphi^c_n(\theta) = \cos n\theta, \quad \varphi^s_n(\theta) = \sin n\theta.$$

The following proposition holds.

Proposition 3.1. *We have*

$$\widetilde{\mathcal{A}}[\varphi^c_n](\zeta) = \sum_{m=1}^{\infty} -\frac{\tilde{r}_2^{-(n+m)}}{4\pi n} (M^{cc}_{nm}(\lambda_{D_1}, \widetilde{D}_1) \cos m\theta + M^{cs}_{nm}(\lambda_{D_1}, \widetilde{D}_1) \sin m\theta), \tag{3.16}$$

and

$$\widetilde{\mathcal{A}}[\varphi^s_n](\zeta) = \sum_{m=1}^{\infty} -\frac{\tilde{r}_2^{-(n+m)}}{4\pi n} (M^{sc}_{nm}(\lambda_{D_1}, \widetilde{D}_1) \cos m\theta + M^{ss}_{nm}(\lambda_{D_1}, \widetilde{D}_1) \sin m\theta) \tag{3.17}$$

for $n \neq 0$.

Proof. Since $\partial \widetilde{D}_2$ is a circle, $\mathcal{K}^*_{\widetilde{D}_2} = 0$ on $\mathcal{H}^*(\partial \widetilde{D}_2)$. Therefore, we only need to consider the second term in $\mathcal{A}$. It is easy to see that

$$\mathcal{S}_{\widetilde{D}_2}\big[\varphi_n^c\big](r,\theta) = -\frac{\tilde{r}_2^{-n+1}}{2n} r^n \cos n\theta, \tag{3.18}$$

$$\mathcal{S}_{\widetilde{D}_2}\big[\varphi_n^s\big](r,\theta) = -\frac{\tilde{r}_2^{-n+1}}{2n} r^n \sin n\theta, \tag{3.19}$$

for $0 \le r \le \tilde{r}_2$. Thus, we have

$$\widetilde{\mathcal{A}}[\varphi_n^c](\zeta) = -\frac{\tilde{r}_2^{-n+1}}{2n}\frac{\partial}{\partial \nu_2}\int_{\partial \widetilde{D}_1} G(\zeta,\zeta')\left(\lambda_{D_1} I - \mathcal{K}^*_{\widetilde{D}_1}\right)^{-1}\left[\frac{\partial}{\partial \nu_1}\mathrm{Re}\{P_n\}\right](\zeta')\, d\sigma(\zeta'). \tag{3.20}$$

It is known that [2]

$$G(x,y) = \sum_{m=1}^{\infty} \frac{(-1)}{2\pi m}\frac{\cos(m\theta_x)}{r_x^m} r_y^m \cos(m\theta_y) + \frac{(-1)}{2\pi m}\frac{\sin(m\theta_x)}{r_x^m} r_y^m \sin(m\theta_y), \quad |x| < |y|,$$

where (r_x,θ_x) and (r_y,θ_y) are the polar coordinates of x and y, respectively. Then, by letting $x = \zeta$ and $y = \zeta' \in \partial \widetilde{D}_2$, we get

$$\begin{aligned}\widetilde{\mathcal{A}}[\varphi_n^c](\zeta) = \sum_{m=1}^{\infty} -\frac{\tilde{r}_2^{-(n+m)}}{4\pi n}\cos m\theta \int_{\partial \widetilde{D}_1} \mathrm{Re}\{P_m\}\left(\lambda_{D_1} I - \mathcal{K}^*_{\widetilde{D}_1}\right)^{-1}\left[\frac{\partial}{\partial \nu_1}\mathrm{Re}\{P_n\}\right](\zeta')\, d\sigma(\zeta') \\ -\frac{\tilde{r}_2^{-(n+m)}}{4\pi n}\sin m\theta \int_{\partial \widetilde{D}_1} \mathrm{Im}\{P_m\}\left(\lambda_{D_1} I - \mathcal{K}^*_{\widetilde{D}_1}\right)^{-1}\left[\frac{\partial}{\partial \nu_1}\mathrm{Re}\{P_n\}\right](\zeta')\, d\sigma(\zeta').\end{aligned}$$

Finally, from the definition of the CGPTs (see (2.13)), (3.16) follows. Similarly, one can derive (3.17). □

Let us define

$$M_{nm} = M_{nm}(\lambda_{D_1}, \widetilde{D}_1) = \begin{pmatrix} M_{nm}^{cc}(\lambda_{D_1}, \widetilde{D}_1) & M_{nm}^{cs}(\lambda_{D_1}, \widetilde{D}_1) \\ M_{nm}^{sc}(\lambda_{D_1}, \widetilde{D}_1) & M_{nm}^{ss}(\lambda_{D_1}, \widetilde{D}_1)\end{pmatrix},$$

and

$$\widetilde{M}_{nm} = -\frac{r_2^{-(n+m)}}{4\pi n} M_{nm}(\lambda_{D_1}, \widetilde{D}_1).$$

In view of Proposition 3.1, we see that the operator $\widetilde{A}$ can be represented in a block matrix form as follows:

$$\widetilde{A} = \begin{bmatrix} \widetilde{M}_{11} & \widetilde{M}_{12} & \widetilde{M}_{13} & \cdots \\ \widetilde{M}_{21} & \widetilde{M}_{22} & \cdots & \cdots \\ \widetilde{M}_{31} & \cdots & \cdots & \\ \cdots & & & \end{bmatrix}. \tag{3.21}$$

Recall that $\widetilde{D}_1$ is contained in the disk $\widetilde{B}_1$ with radius $\tilde{r}_1$. One can derive that

$$|M_{nm}(\lambda_{D_1}, \widetilde{D}_1)| \le C\tilde{r}_1^{n+m}$$

for some positive constant C [4]. Therefore,

$$|\widetilde{M}_{nm}(\lambda_{D_1}, \widetilde{D}_1)| \leq C \left(\frac{\tilde{r}_1}{\tilde{r}_2}\right)^{n+m}. \tag{3.22}$$

This decay property of $\widetilde{M}_{nm}$ is crucial for our conformal mapping technique. An important consequence is that the operator $\widetilde{\mathcal{A}}$ can be efficiently approximated by finite dimensional matrices obtained through a standard truncation procedure. Here we remark that $\widetilde{\mathcal{A}} = O((\tilde{r}_1/\tilde{r}_2)^2)$.

If the particle D_1 is in the strong regime, then we may write $d = c\delta$ for some $c > 0$. If c is of order one, the ratio $\frac{\tilde{r}_1}{\tilde{r}_2}$ is relatively small (but regardless of how small δ is). In section 4 we apply the eigenvalue perturbation method to analyze the spectral nature more explicitly when we consider the related inverse problem.

3.5 Spectral decomposition $\mathcal{A}$ of and the scattered field

It is clear that $\widetilde{\mathcal{A}}$ is compact and is self-adjoint in $\mathcal{H}^*$. Let $\{(\lambda_n, \widetilde{\psi}_n) : n \geq 1\}$ be the set of its eigenvalue-eigenfunction pairs. We order the eigenvalues in such a way that $|\lambda_j|$ is decreasing and tends to 0 as $j \to \infty$. Then $\mathcal{A}$ admits the following spectral decomposition:

$$\widetilde{\mathcal{A}} = \sum_{n=1}^{\infty} \lambda_j \widetilde{\psi}_n \otimes \widetilde{\psi}_n.$$

We remark that all the eigenvalues $\{\lambda_j : j \geq 1\}$ lie in the interval $(-1/2, 1/2)$. Moreover, they can be numerically approximated by the eigenvalues of a finite truncation of the infinite matrix $\widetilde{\mathcal{A}}$.

Thanks to (3.15), if we let $\psi_n = \widetilde{\psi}_n \circ \Phi$, then we obtain

$$\mathcal{A} = \sum_{n=1}^{\infty} \lambda_j \psi_n \otimes \psi_n. \tag{3.23}$$

It is also worth mentioning that the orthogonality of basis $\{\psi_n\}$ is also preserved.

Using the spectral representation formula (3.23), we can derive the following result.

Theorem 3.1. *Assume that Condition 1 holds and that D_2 is in the strong interaction regime, then the scattered field $u^s_{D_2} = u - u_{D_1}$ by the plasmonic particle D_2 has the following representation:*

$$u^s_{D_2} = \mathcal{S}_{D_2,D_1}[\psi],$$

where ψ satisfies

$$\psi = \sum_{j=1}^{\infty} \frac{\left(\nabla u^i(z) \cdot \nu, \psi_j\right)_{\mathcal{H}^*(\partial D_2)} \psi_j + O(\delta^2)}{\lambda_{D_2} - \lambda_j}.$$

As a corollary, we obtain the following asymptotic expansion of the scattered field $u - u^i$.

Theorem 3.2. *The following far field expansion holds:*

$$(u - u^i)(x) = \nabla u^i(z) \cdot M(\lambda_{D_1}, \lambda_{D_2}, D_1, D_2) \nabla G(x, z) + O\left(\frac{\delta^3}{\mathrm{dist}(\lambda_{D_2}, \sigma(\mathcal{A}))} \frac{1}{|x|^2} \right),$$

as $|x| \to \infty$. Here, z is the center of mass of D_2 and $M(\lambda_{D_1}, \lambda_{D_2}, D_1, D_2)$ is the polarization tensor satisfying

$$M(\lambda_{D_1}, \lambda_{D_2}, D_1, D_2)_{l,m} = \sum_{j=1}^{\infty} \frac{(\nu_l, \psi_j)_{\mathcal{H}^*(\partial D_2)} (\psi_j, x_m)_{-\frac{1}{2},\frac{1}{2}} + O(\delta^2)}{\lambda_{D_2} - \lambda_j}, \tag{3.24}$$

for $l, m = 1, 2$.

From the above far field expansion of the scattered field, it is clear that when we vary the frequency of the incident field, at certain frequency ω such that $\lambda_{D_2}(\omega) = \lambda_j$ for some j which satisfies the condition that

$$(\nu_l, \psi_j)_{\mathcal{H}^*(\partial D_2)} (\psi_j, x_m)_{-\frac{1}{2},\frac{1}{2}} \neq 0,$$

the scattered field will show a sharp peak, which corresponds to the excitation of a plasmonic resonance. Such a frequency is called a plamonic resonant frequency for the system of two particles, which is different from the one for the single plasmonic particle D_2. The difference is called the shift of resonant frequency. This shift is due to the interaction of the target particle with the plasmonic particle. We note that the resonant frequencies of the two-particle system can be determined from the far field data, which further determines those λ_j which are eigenvalues of the operator $\mathcal{A}$. In the next section, we discuss how to reconstruct the shape of D_1 from these recovered eigenvalues.

4 The inverse problem

We assume that we can measure the eigenvalues λ_j for $j = 1, 2, ..., J$, from the far field by varying the frequency of incident field and then picking up local peaks. These eigenvalues are also the eigenvalues of the operator $\widetilde{\mathcal{A}}$, which depends on the CGPTs of the transformed shape $\widetilde{D}_1$ according to (3.21). So we reconstruct $\widetilde{D}_1$ first. Once we find $\widetilde{D}_1$, the shape of D_1 can be easily recovered by using the mapping Φ.

4.1 Reconstruction of CGPTs

In this subsection, we propose an algorithm to reconstruct the CGPTs from measurements of the eigenvalues λ_j. For ease of presentation, we only consider the first two largest eigenvalues λ_1 and λ_2. We denote their measurements by $\mathcal{P}_1$ and $\mathcal{P}_2$, respectively. Note that a single measurement of $(\mathcal{P}_1, \mathcal{P}_2)$ typically yields very poor reconstruction of the CGPTs due to the lack of information. To overcome this issue, we need to measure the eigenvalues for different configurations of the two particles. Recall the target particle contains the origin. We can rotate it around the origin multiple times and measure $(\mathcal{P}_1, \mathcal{P}_2)$ for each configuration. The CGPTs for the target particle after each rotation are related in the following way.

Define

$$N^{(1)}_{m,n}(\lambda, D) = (M^{cc}_{m,n} - M^{ss}_{m,n}) + i(M^{cs}_{m,n} + M^{sc}_{m,n}),$$
$$N^{(2)}_{m,n}(\lambda, D) = (M^{cc}_{m,n} + M^{ss}_{m,n}) + i(M^{cs}_{m,n} - M^{sc}_{m,n})$$

and let $R_\theta D = \{e^{i\theta}x : x \in D\}, \theta \in [0, 2\pi)$. Then for all integers m, n and all angle parameters θ, we have [2]

$$N^{(1)}_{m,n}(R_\theta D) = e^{i(n+m)\theta} N^{(1)}_{m,n}(D), \quad N^{(2)}_{m,n}(R_\theta D) = e^{i(n-m)\theta} N^{(2)}_{m,n}(D).$$

Let us write $d = c\delta$ for some $c > 0$. As discussed in subsection 3.2, if c is of order one, then the deformation of the shape $\widetilde{D}_1$ from D_1 is not so strong. So, if the domain D_1 is rotated by an angle θ, then the transformed domain will also be rotated by the same amount of angle. So we may (approximately) identify $\widetilde{R_\theta D_1}$ with $R_\theta \widetilde{D}_1$.

Measuring $\mathcal{P}_j$ for multiple rotation angles θ_i for $R_\theta \widetilde{D}_1$ will yield a non-linear system of equations that will allow the recovery of the CGPTs associated with D_1. From the recovered CGPTs, we will reconstruct the ordinary particle D_1. Here, we only consider the shape reconstruction problem. Nevertheless, by using the CGPTs associated with D_1, it is possible to reconstruct the permittivity ε_1 of D_1 in the case it is not a priori given [2].

In view of (3.21) and (3.22), using a standard perturbation method, the asymptotic expansion of the eigenvalue $\lambda_j, j = 1, 2$

$$\lambda_j = \lambda_j^0 + \lambda_j^1 + \lambda_j^2 + \cdots, \quad \text{where } \lambda_j^k = O\big((\tilde{r}_1/\tilde{r}_2)^{k+2} \big) \tag{4.1}$$

for $i = 1, 2$. Each term in the RHS of the above expansion can be computed explicitly. Although we omit the explicit expressions, we mention that they are nonlinear and depend on CGPTs in the following way:

$$\begin{aligned}
\lambda_j^0 &= \lambda_j^0(M_{11}), \\
\lambda_j^1 &= \lambda_j^1(M_{11}, M_{12}), \\
\lambda_j^2 &= \lambda_j^2(M_{11}, M_{12}, M_{22}, M_{13}), \\
\vdots &= \qquad \vdots \\
\lambda_j^k &= \lambda_j^k(\cup_{m+n \le k+2}\{M_{mn}\}).
\end{aligned}$$

Suppose we have measurements $\mathcal{P}_1(\theta)$ and $\mathcal{P}_2(\theta)$ for 11 different rotation angles $\theta_1, \theta_2, ..., \theta_{11}$ of the unknown particle $\widetilde{D}_1$. We can reconstruct M_{nm} approximately for $m + n \le 5$. Recall that $M_{mn} = M^T_{nm}$ where subscript T stands for the transpose. We look for a set of matrices

$\{M^{(1)}_{nm}\}_{m+n\leq 5}$ satisfying $[M^{(1)}_{nm}]^T = M^{(1)}_{mn}$ and the the following nonlinear system: for $j = 1, 2$,

$$\begin{aligned}
\mathcal{P}_j(\theta_1) &= \sum_{l=0}^{3} \lambda_j^l \Big(\cup_{m+n\leq l+2} \{M^{(1)}_{nm}(R_{\theta_1}\widetilde{D}_1)\}\Big), \\
\mathcal{P}_j(\theta_2) &= \sum_{l=0}^{3} \lambda_j^l \Big(\cup_{m+n\leq l+2} \{M^{(1)}_{nm}(R_{\theta_2}\widetilde{D}_1)\}\Big), \\
\vdots &= \qquad \vdots \\
\mathcal{P}_j(\theta_{11}) &= \sum_{l=0}^{3} \lambda_j^l \Big(\cup_{m+n\leq l+2} \{M^{(1)}_{nm}(R_{\theta_{11}}\widetilde{D}_1)\}\Big).
\end{aligned}$$

We note that the above equations has 22 independent parameters. They can be solved by using standard optimization methods. We expect that

$$M_{nm} = M^{(1)}_{nm} + O\big((\tilde{r}_1/\tilde{r}_2)^6 \big) \quad \text{for } m+n \leq 5.$$

The above scheme can be easily generalized to reconstruct the higher order CGPTs M_{nm}. This requires more measurement data $(\mathcal{P}_1, \mathcal{P}_2)$ from more rotations. Let $k \geq 2$. One can see that (using the symmetry $[M^{(k)}_{nm}]^T = M^{(k)}_{mn}$) the set of GPTs M_{mn} satisfying $m+n \leq 4k+1$ contains e_k independent parameters, where e_k is given by

$$e_k = 16k^2 + 6k.$$

Therefore, we need $e_k/2$ pairs of $(\mathcal{P}_1, \mathcal{P}_2)$ to reconstruct these GPTs. Let $\{M^{(k)}_{nm}\}_{m+n\leq 4k+1}$ be the set of matrices satisfying $[M^{(k)}_{nm}]^T = M^{(k)}_{mn}$ and the following system of equations:

$$\mathcal{P}_j(\theta_i) = \sum_{l=0}^{k-1} \lambda_j^l \Big(\cup_{m+n\leq l+2} \{M^{(k)}_{nm}(R_{\theta_i}\widetilde{D}_1)\}\Big), \quad i = 1, ..., e_k, \ j = 1, 2.$$

Then we have

$$M_{nm} = M^{(k)}_{nm} + O\big((\tilde{r}_1/\tilde{r}_2)^{4k+2} \big) \quad \text{for } m+n \leq 4k+1.$$

4.2 Optimal control approach

Now, in order to recover the shape of $\widetilde{D}_1$ from the CGPTs M_{mn}, we can minimize the following energy functional

$$\mathcal{J}_c^{(l)}[B] := \frac{1}{2} \sum_{H,F\in\{c,s\}} \sum_{n+m\leq k} \left| M^{HF}_{mn}(\lambda_{D_1}, B) - M^{HF}_{mn}(\lambda_{D_1}, D_1) \right|^2 , \tag{4.2}$$

We apply the gradient descent method for the minimization. We need the shape derivative of the functional $\mathcal{J}_c^{(l)}[B]$. For ϵ small, let B_ϵ be an ϵ-deformation of B, *i.e.*, there is a scalar function $h \in \mathcal{C}^1(\partial B)$, such that

$$\partial B_\epsilon := \{x + \epsilon h(x)\nu(x) \ : x \in \partial B\}.$$

According to [2, 3, 6], the perturbation of the CGPTs due to the shape deformation is given by

$$
\begin{aligned}
& M_{nm}^{HF}(\lambda_{D_1}, B_\epsilon) - M_{nm}^{HF}(\lambda_{D_1}, B) \\
& \quad = \epsilon(k_{\lambda_{D_1}} - 1) \int_{\partial B} h(x) \left[\frac{\partial u}{\partial \nu}\Big|_- \frac{\partial v}{\partial \nu}\Big|_- + \frac{1}{k_{\lambda_{D_1}}} \frac{\partial u}{\partial T}\Big|_- \frac{\partial v}{\partial T}\Big|_- \right](x)\, d\sigma(x) + O(\epsilon^2),
\end{aligned} \tag{4.3}
$$

where

$$
k_{\lambda_{D_1}} = (2\lambda_{D_1} + 1)/(2\lambda_{D_1} - 1), \tag{4.4}
$$

and u and v are respectively the solutions to the following transmission problems:

$$
\begin{cases}
\Delta u = 0 & \text{in } B \cup (\mathbb{R}^2 \setminus \overline{B}) \ , \\
u|_+ - u|_- = 0 & \text{on } \partial B \ , \\
\dfrac{\partial u}{\partial \nu}\Big|_+ - k_{\lambda_{D_1}} \dfrac{\partial u}{\partial \nu}\Big|_- = 0 & \text{on } \partial B \ , \\
(u - H)(x) = O(|x|^{-1}) & \text{as } |x| \to \infty \ ,
\end{cases} \tag{4.5}
$$

and

$$
\begin{cases}
\Delta v = 0 & \text{in } B \cup (\mathbb{R}^2 \setminus \overline{B}) \ , \\
k_{\lambda_{D_1}} v|_+ - v|_- = 0 & \text{on } \partial B \ , \\
\dfrac{\partial v}{\partial \nu}\Big|_+ - \dfrac{\partial v}{\partial \nu}\Big|_- = 0 & \text{on } \partial B \ , \\
(v - F)(x) = O(|x|^{-1}) & \text{as } |x| \to \infty \ .
\end{cases} \tag{4.6}
$$

Here, $\partial/\partial T$ is the tangential derivative. In the case of M_{nm}^{cs}, for example, we put $H = \mathrm{Re}\{P_n\} = r^n \cos n\theta$ and $F = \mathrm{Im}\{P_m\} = r^n \sin n\theta$. The other cases can be handled similarly.

Let

$$
w_{m,n}^{HF}(x) = (k_{\lambda_{D_1}} - 1) \left[\frac{\partial u}{\partial \nu}\Big|_- \frac{\partial v}{\partial \nu}\Big|_- + \frac{1}{k_{\lambda_{D_1}}} \frac{\partial u}{\partial T}\Big|_- \frac{\partial v}{\partial T}\Big|_- \right](x), \quad x \in \partial B \ .
$$

The shape derivative of $\mathcal{J}_c^{(l)}$ at B in the direction of h is given by

$$
\langle d_S \mathcal{J}_c^{(l)}[B], h \rangle = \sum_{H,F \in \{c,s\}} \sum_{m+n \leq k} \delta_N^{HF} \langle w_{m,n}^{HF}, h \rangle_{L^2(\partial B)} \ ,
$$

where

$$
\delta_N^{HF} = M_{nm}^{HF}(\lambda_{D_1}, B) - M_{nm}^{HF}(\lambda_{D_1}, D_1) \ .
$$

By using the shape derivatives of the CGPTs, we can get an approximation for the matrix $\big(\widetilde{M}_{nm}(\lambda_{D_1}, B_\epsilon)\big)_{n,m=1}^N$ for the slightly deformed shape. Next, the shape derivative of $\lambda_j^N(B)$ can be computed by using the standard eigenvalue perturbation theory. Finally, by applying a gradient descent algorithm, we can minimize, at least locally, the energy functional $\mathcal{J}_c^{(l)}$.

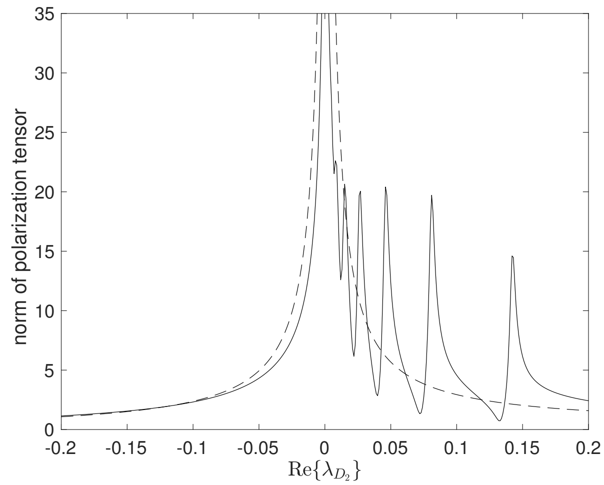

Figure 3: The magnitude of the polarization tensor. The dotted line (or solid line) represents the case when the dieletric particle D_1 is absent (or presented), respectively. We set $\mathrm{Im}\{\lambda_2\} = 0.003$.

4.3 Numerical examples

In this subsection, we support our theoretical results by numerical examples. In the sequel, we set $\delta = 0.001$. We also assume that B_1 and B_2 are disks of radii $r_1 = \delta$ and $r_2 = 1$, respectively and they are separated by a distance $d = 5\delta$. Then the ratio $\tilde{r}_1/\tilde{r}_2$ between the trasnformed radii is approximately 0.127. Note that the ratio is rather small but much larger than the small parameter δ. We suppose the material parmater ε_1 of D_1 is known and to be given by $\varepsilon_1 = 3$ and so, it holds that $\lambda_{D_1} = 1$.

We rotate the unknown particle D_1 by the angle $\theta_i, i = 1, 2, ..., 11$ and get the measurement pair $(\mathcal{P}_1(\theta_i), \mathcal{P}_2(\theta_i))$ for each rotation θ_i, where θ_i is given by

$$\theta_i = \frac{2\pi}{11}(i-1), \quad i = 1, 2, ..., 11.$$

We mention that, as discussed in [10], we can measure $(\mathcal{P}_1, \mathcal{P}_2)$ from the local peaks of the plasmonic resonant far-field.

Figure 3 shows the shift in the plasmonic resonance. In the absence of the dielectric particle D_1, the local peak occurs only at $\lambda_{D_2} = 0$. If the particle D_1 is presented in a strong regime, then many local peaks appear. By measuring the first two largest values of λ_{D_2} at which a local peak appear, we get $(\mathcal{P}_1, \mathcal{P}_2)$ approximately.

From measurements of $(\mathcal{P}_1, \mathcal{P}_2)$, we recover the contracted GPTs using the algorithm described in subsection 4.1. We then minimize functional (4.2) to reconstruct an approximation of $\widetilde{D}_1$. Finally, we use $D_1 = \Phi^{-1}(\widetilde{D}_1)$ to get the shape of D_1. We consider the case of D_1 being a flower-shaped particle and show comparison between the target shapes and the reconstructed ones, as shown in Figure 4. We recover the first contracted GPTs up to order 5, *i.e.*, M_{mn} for $m + n \leq 5$. We take as an initial guess the equivalent ellipse to $\widetilde{D}_1$, determined from the recovered first order polarization tensor. The required number of iterations is 30. It is clear that they are in good agreement.

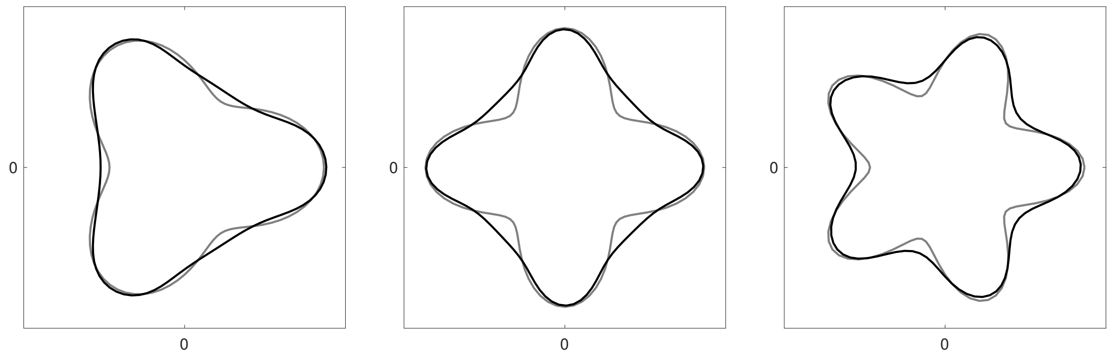

Figure 4: Comparison between the original shape (gray) of the particle D_1 and the reconstructed one (black). The iteration number is 30.

References

[1] H. Ammari, Y. Deng, and P. Millien, Surface plasmon resonance of nanoparticles and applications in imaging, Arch. Ration. Mech. Anal., 220 (2016), 109–153.

[2] H. Ammari, J. Garnier, W. Jing, H. Kang, M. Lim, K. Sølna, and H. Wang, *Mathematical and Statistical Methods for Multistatic Imaging*, Lecture Notes in Mathematics, Volume 2098, Springer, Cham, 2013.

[3] H. Ammari, J. Garnier, H. Kang, M. Lim, and S. Yu, Generalized polarization tensors for shape description, Numer. Math., 126 (2014), 199–224.

[4] H. Ammari and H. Kang, Polarization and Moment Tensors with Applications to Inverse Problems and Effective Medium Theory, Applied Mathematical Sciences, Vol. 162, Springer-Verlag, New York, 2007.

[5] H. Ammari and H. Kang, Generalized polarization tensors, inverse conductivity problems, and dilute composite materials: a review, Contemporary Mathematics, Volume 408 (2006), 1–67.

[6] H. Ammari, H. Kang, M. Lim, and H. Zribi, The generalized polarization tensors for resolved imaging. Part I: Shape reconstruction of a conductivity inclusion, Math. Comp., 81 (2012), 367–386.

[7] H. Ammari, P. Millien, M. Ruiz, and H. Zhang, Mathematical analysis of plasmonic nanoparticles: the scalar case, Archive on Rational Mechanics and Analysis, 224 (2017), 597-658.

[8] H. Ammari, M. Putinar, M. Ruiz, S. Yu, and H. Zhang, Shape reconstruction of nanoparticles from their associated plasmonic resonances, J. Math. Pures Appl., DOI:10.1016/j.matpur.2017.09.003, to appear.

[9] H. Ammari, M. Ruiz, S. Yu, and H. Zhang, Mathematical analysis of plasmonic resonances for nanoparticles: the full Maxwell equations, Journal of Differential Equations, 261 (2016), 3615-3669.

[10] H. Ammari, M. Ruiz, S. Yu, and H. Zhang, Reconstructing fine details of small objects by using plasmonic spectroscopic data, SIAM J. Imag. Sci., to appear.

[11] H. Ammari and H. Zhang, A mathematical theory of super-resolution by using a system of sub-wavelength Helmholtz resonators, Comm. Math. Phys., 337 (2015), 379–428.

[12] H. Ammari and H. Zhang, Super-resolution in high contrast media, Proc. Royal Soc. A, 2015 (471), 20140946.

[13] H. Ammari and H. Zhang, Effective medium theory for acoustic waves in bubbly fluids near Minnaert resonant frequency, SIAM J. Math. Anal., 49 (2017), 3252–3276.

[14] K. Ando and H. Kang, Analysis of plasmon resonance on smooth domains using spectral properties of the Neumann-Poincaré operator, J. Math. Anal. Appl., 435 (2016), 162–178.

[15] K. Ando, H. Kang, and H. Liu, Plasmon resonance with finite frequencies: a validation of the quasi-static approximation for diametrically small inclusions, SIAM J. Appl. Math., 76 (2016), 731–749.

[16] G. Baffou, C. Girard, and R. Quidant, Mapping heat origin in plasmonic structures, Phys. Rev. Lett., 104 (2010), 136805.

[17] M. Reed and B. Simon, *Methods of Modern Mathematical Physics. IV Analysis of Operators*, Academic Press, New York, 1970.

[18] M. Fatemi, A. Amini, and M. Vetterli, Sampling and reconstruction of shapes with algebraic boundaries, IEEE Trans. Signal Proc., 64 (2016), 5807–5818.

[19] D. Grieser, The plasmonic eigenvalue problem, Rev. Math. Phys., 26 (2014), 1450005.

[20] P.K. Jain, K.S. Lee, I.H. El-Sayed, and M.A. El-Sayed, Calculated absorption and scattering properties of gold nanoparticles of different size, shape, and composition: Applications in biomedical imaging and biomedicine, J. Phys. Chem. B, 110 (2006), 7238–7248.

[21] M. I. Gil, Norm Estimations for Operator Valued Functions and Applications, Vol. 192. CRC Press, 1995.

[22] K.L. Kelly, E. Coronado, L.L. Zhao, and G.C. Schatz, The optical properties of metal nanoparticles: The influence of size, shape, and dielectric environment, J. Phys. Chem. B, 107 (2003), 668–677.

[23] S. Link and M.A. El-Sayed, Shape and size dependence of radiative, non-radiative and photothermal properties of gold nanocrystals, Int. Rev. Phys. Chem., 19 (2000), 409–453.

[24] I.D. Mayergoyz, D.R. Fredkin, and Z. Zhang, Electrostatic (plasmon) resonances in nanoparticles, Phys. Rev. B, 72 (2005), 155412.

[25] O.D. Miller, C.W. Hsu, M.T.H. Reid, W. Qiu, B.G. DeLacy, J.D. Joannopoulos, M. Soljacić, and S. G. Johnson, Fundamental limits to extinction by metallic nanoparticles, Phys. Rev. Lett., 112 (2014), 123903.

[26] M. Minnaert, On musical air-bubbles and the sounds of running water. The London, Edinburgh, Dublin Philos. Mag. and J. of Sci., 16 (1933), 235–248.

[27] D. Sarid and W. A. Challener, *Modern Introduction to Surface Plasmons: Theory, Mathematical Modeling, and Applications*, Cambridge University Press, New York, 2010.

[28] L.B. Scaffardi and J.O. Tocho, Size dependence of refractive index of gold nanoparticles, Nanotech., 17 (2006), 1309–1315.

[29] J. Yang, H. Giessen, and P. Lalanne, Simple analytical expression for the peak-frequency shifts of plasmonic resonances for sensing, Nano Lett., 15 (2015), 3439–3444.

[30] J. N. Anker, W. P. Hall, O. Lyandres, N. C. Shah, J. Zhao, and R. P. Van Duyne, Biosensing with plasmonic nanosensors, Nature material, 7 (2008), 442–453.